Biogeosciences Discuss., 12, 17009–17049, 2015
www.biogeosciences-discuss.net/12/17009/2015/
doi:10.5194/bgd-12-17009-2015

Biogeosciences Discussions
Open Access
EGU

The mechanism of oxygen isotope fractionation during N_2O production by denitrification

D. Lewicka-Szczebak[1], J. Dyckmans[2], J. Kaiser[3], A. Marca[3], J. Augustin[4], and R. Well[1]

[1]Thünen Institute of Climate-Smart Agriculture, Federal Research Institute for Rural Areas, Forestry and Fisheries, Bundesallee 50, 38116 Braunschweig, Germany
[2]Centre for Stable Isotope Research and Analysis, University of Göttingen, Büsgenweg 2, 37077 Göttingen, Germany
[3]Centre for Ocean and Atmospheric Sciences, School of Environmental Sciences, University of East Anglia, Norwich, NR4 7TJ, UK
[4]Leibniz Centre for Agricultural Landscape Research, Eberswalder Straße 84, 15374 Müncheberg, Germany

Received: 15 September 2015 – Accepted: 9 October 2015 – Published: 22 October 2015

Correspondence to: D. Lewicka-Szczebak (dominika.lewicka@ti.bund.de)

Published by Copernicus Publications on behalf of the European Geosciences Union.

Abstract

The isotopic composition of soil-derived N_2O can help differentiate between N_2O production pathways and estimate the fraction of N_2O reduced to N_2. Until now, $\delta^{18}O$ of N_2O has been rarely used in the interpretation of N_2O isotopic signatures because of the rather complex oxygen isotope fractionations during N_2O production by denitrification. The latter process involves nitrate reduction mediated through the following three enzymes: nitrate reductase (NAR), nitrite reductase (NIR) and nitric oxide reductase (NOR). Each step removes one oxygen atom as water (H_2O), which gives rise to a branching isotope effect. Moreover, denitrification intermediates may partially or fully exchange oxygen isotopes with ambient water, which is associated with an exchange isotope effect. The main objective of this study was to decipher the mechanism of oxygen isotope fractionation during N_2O production by denitrification and, in particular, to investigate the relationship between the extent of oxygen isotope exchange with soil water and the $\delta^{18}O$ values of the produced N_2O.

We performed several soil incubation experiments. For the first time, $\Delta^{17}O$ isotope tracing was applied to simultaneously determine the extent of oxygen isotope exchange and any associated oxygen isotope effect. We found bacterial denitrification to be typically associated with almost complete oxygen isotope exchange and a stable difference in $\delta^{18}O$ between soil water and the produced N_2O of $\delta^{18}O(N_2O / H_2O) = (17.5 \pm 1.2)$ ‰. However, some experimental setups yielded oxygen isotope exchange as low as 56 % and a higher $\delta^{18}O(N_2O / H_2O)$ of up to 37 ‰. The extent of isotope exchange and $\delta^{18}O(N_2O / H_2O)$ showed a very significant correlation ($R^2 = 0.70$, $p < 0.00001$). We hypothesise that this observation was due to the contribution of N_2O from another production process, most probably fungal denitrification.

An oxygen isotope fractionation model was used to test various scenarios with different magnitudes of branching isotope effects at different steps in the reduction process. The results suggest that during denitrification the isotope exchange occurs prior to the isotope branching and that the mechanism of this exchange is mostly associated

BGD
12, 17009–17049, 2015

with the enzymatic nitrite reduction mediated by NIR. For bacterial denitrification, the branching isotope effect can be surprisingly low, about (0.0 ± 0.9) ‰; in contrast to fungal denitrification where higher values of up to 30 ‰ have been reported previously. This suggests that $\delta^{18}O$ might be used as a tracer for differentiation between bacterial and fungal denitrification, due to their different magnitudes of branching isotope effects.

1 Introduction

Our ability to mitigate soil N_2O emissions is limited due to poor understanding of the complex interplay between N_2O production pathways in soil environments. In order to develop effective fertilizing strategies and reduce the loss of nitrogen through microbial consumption as well as related adverse environmental impacts, it is very important to fill the existing knowledge gaps. Isotopocule analyses of N_2O, including $\delta^{18}O$, average $\delta^{15}N$ ($\delta^{15}N^{av}$) and ^{15}N site preference within the linear N_2O molecule ($\delta^{15}N^{sp}$) have been used for several years to help differentiate between N_2O production pathways (Opdyke et al., 2009; Perez et al., 2006; Sutka et al., 2006; Toyoda et al., 2005; Well et al., 2008), the various microbes involved (Rohe et al., 2014a; Sutka et al., 2008, 2003) and to estimate the magnitude of N_2O reduction to N_2 (Ostrom et al., 2007; Park et al., 2011; Toyoda et al., 2011; Well and Flessa, 2009). However, the usefulness of these analyses would be enhanced further if the isotope fractionation mechanisms were better understood. In particular, we need to know the isotope fractionations associated with nitrate and N_2O reduction to quantify the fraction of N_2O reduced to N_2 based on the N_2O isotopic signatures (Lewicka-Szczebak et al., 2014, 2015). This would be most effective if either of the isotopic signatures ($\delta^{18}O$, $\delta^{15}N^{av}$ or $\delta^{15}N^{sp}$) were stable or predictable for N_2O produced by each of the relevant processes (e.g. heterotrophic bacterial denitrification, fungal denitrification, nitrifier denitrification and nitrification). We hypothesize that this could be the case for $\delta^{18}O$, which was the focus of this study.

BGD
12, 17009–17049, 2015

$\delta^{18}O$ of N_2O has been rarely applied in the interpretation of N_2O isotopic signatures because of the rather complex oxygen isotope fractionations during N_2O production by denitrification (Kool et al., 2007). It is controlled by the origin of the oxygen atom in the N_2O molecule (nitrate, nitrite, soil water or molecular O_2) and by the isotope fractionation during nitrate reduction or during oxygen isotope exchange with soil water. N_2O production during denitrification is a stepwise process of nitrate reduction mediated by the following three enzymes: nitrate reductase (NAR), nitrite reductase (NIR) and nitric oxide reductase (NOR) (Kool et al., 2007) as presented in the simplified scheme in Fig. 1. During each reduction step, one oxygen atom is detached and removed as water (H_2O), which is associated with branching isotope effects (Casciotti et al., 2007; Snider et al., 2013). Conceptually, these can be regarded as a combination of two isotope fractionations with opposite effects on the $\delta^{18}O$ signature of the reduction product: (i) intermolecular fractionation due to preferential reduction of ^{18}O-depleted molecules, which results in ^{18}O-enriched residual substrate and ^{18}O-depleted product, and (ii) intramolecular fractionation due to preferential ^{16}O abstraction, which results in ^{18}O-enriched nitrogen-bearing reduction products and ^{18}O-depleted H_2O as side product. Since intermolecular fractionation causes ^{18}O depletion of the reduction product and intramolecular fractionation causes ^{18}O enrichment, the net branching effect (ε_n) can theoretically vary between negative and positive values. However, pure cultures studies show that ε_n is mostly positive, i.e. between 25 and 30 ‰ for bacterial denitrification (Casciotti et al., 2007) and between 10 and 30 ‰ for fungal denitrification (Rohe et al., 2014a).

Moreover, denitrification intermediates may partially or fully exchange oxygen isotopes with ambient water (Kool et al., 2009). The isotopic signature of the incorporated O-atom depends on the isotopic signature of ambient water and the isotope fractionation associated with this exchange. Under typical soil conditions, i.e. pH close to neutral and moderate temperatures, abiotic isotope exchange between nitrate and water is negligibly slow. In extremely acid conditions (pH < 0), the equilibrium effect is $\varepsilon(NO_3^-/H_2O)$ = 23 ‰ (Böhlke et al., 2003). Casciotti et al. (2007) showed that for nitrite

BGD
12, 17009–17049, 2015

the abiotic exchange can also take place at neutral pH, but for achieving an isotopic equilibrium over 8 months are needed. The observed isotope equilibrium effect between nitrite and water is ε (NO_2^-/H_2O) = 14 ‰ at 21 °C. Nothing is known yet about the possible abiotic exchange between NO and ambient water.

The isotope exchange between denitrification intermediates and ambient water is most probably accelerated by enzymatic catalysis, since numerous ^{18}O tracer studies documented nearly complete O isotope exchange (Kool et al., 2009; Rohe et al., 2014b; Snider et al., 2013) within short incubation times like a few hours. Hence, it can be assumed that at least one enzymatic step must be responsible for exchange of O isotopes with soil water (Rohe et al., 2014a; Snider et al., 2013). Consequently, the final $\delta^{18}O$ of produced N_2O may vary over a wide range, depending on the extent of isotope exchange with soil water associated with particular enzyme (Rohe et al., 2014a).

Pure culture studies indicated large differences between various denitrifying microbes. The extent of oxygen isotope exchange ranged from 4 to 100 % for bacterial denitrification (Kool et al., 2007) and from 11 to 100 % for fungal denitrification (Rohe et al., 2014b). In contrast, unsaturated soil incubation experiments, with a natural whole microbial community, showed consistently high magnitudes of O isotope exchange between 85 and 99 % (Kool et al., 2009; Lewicka-Szczebak et al., 2014; Snider et al., 2013). If the high extent of isotope exchange was characteristic of soil denitrification processes, we would expect quite stable $\delta^{18}O$ values of the produced N_2O during denitrification, provided that these values are not influenced by N_2O reduction.

It is difficult to quantitatively link isotope exchange and apparent isotope effects, because using the ^{18}O tracer technique to quantify isotope exchange prevents simultaneous study of isotope oxygen fractionation. However, two studies that conducted parallel ^{18}O traced and natural abundance experiments allowed the authors to propose the first general oxygen isotope fractionation models (Rohe et al., 2014a; Snider et al., 2013). These models showed that the magnitude of overall isotope fractionation depends not only on the overall extent of oxygen isotope exchange but also on the enzymatic re-

BGD
12, 17009–17049, 2015

duction step when it occurs (Fig. 1). Fungi and bacteria are characterized by different NOR mechanisms (Schmidt et al., 2004; Stein and Yung, 2003), which result in distinct $\delta^{15}N^{sp}$ values for bacterial and fungal denitrification. It can be assumed that these differences in NOR also influence $\delta^{18}O$, but this hypothesis has not been tested yet.

In the present study, we used ^{17}O as tracer to determine the extent of O isotope exchange. We applied a nitrate fertilizer of natural atmospheric deposition origin with high ^{17}O excess, as a result of non-random oxygen isotope distribution. Then we measured ^{17}O excess of the produced N_2O and, based on the observed loss of ^{17}O excess, calculated the extent of isotope exchange with water. Simultaneously, we could measure the $^{18}O/^{16}O$ fractionation in the same incubation vessels, since the ^{17}O tracing method has no impact on $\delta^{18}O$. This is the first time that such an approach has been used and to validate this method, we applied an alternative approach. Namely, soil water with distinct $\delta^{18}O$ values within the range of natural abundance isotopic signatures was applied to quantify isotope exchange (Snider et al., 2009).

The latter method has also been applied in a recent soil incubation study (Lewicka-Szczebak et al., 2014) and indicated almost complete oxygen isotope exchange with soil water associated with a stable isotope ratio difference between soil water and produced N_2O of $\delta^{18}O(N_2O/H_2O) = (19.0 \pm 0.7)$ ‰. However, the results of other experiments presented in the same study (Lewicka-Szczebak et al., 2014) indicated much higher $\delta^{18}O(N_2O/H_2O)$ values of up to 42 ‰. The higher values may be due to a lower extent of oxygen isotope exchange, but no data were available for the extent of exchange for those samples. Interestingly, a tight correlation was found between $\delta^{18}O(N_2O/H_2O)$ and soil moisture (Lewicka-Szczebak et al., 2014), suggesting that the extent of isotope exchange may be influenced by soil moisture. In the present study, this hypothesis has been tested with experimental results of soil incubations with three different soil moisture levels.

The isotope fractionation associated with oxygen isotope exchange is expected to be temperature-dependent, but this assumption has never been tested. Hence, in this

BGD
12, 17009–17049, 2015

study we used incubations at two different temperatures to check the temperature dependence.

The combination of various experimental approaches allowed us to further improve the $\delta^{18}O$ fractionation model proposed by Snider et al. (2013) and Rohe et al. (2014a), to decipher the mechanism of oxygen isotope fractionation during N_2O production by denitrification and to determine the associated isotope effects. We investigated the variability of isotope exchange with soil water and of the $\delta^{18}O$ values of produced N_2O under varying conditions as well as the relation between these quantities. Ultimately, our aim was to check to what level of accuracy $\delta^{18}O$ can be predicted based on the known controlling factors. Additionally, the ^{17}O analyses of N_2O produced by denitrification gave us the opportunity to check the hypothesis of soil denitrification contributing to the non-random distribution of oxygen isotopes (^{17}O excess, or $\Delta^{17}O$) in atmospheric N_2O (Kaiser et al., 2004; Michalski et al., 2003).

2 Methods

2.1 Experimental set-ups

2.1.1 Experiment 1 (Exp 1) – static anoxic incubation

The static incubations were performed under an anoxic atmosphere (N_2) in closed vessels where denitrification products accumulated in the headspace. Two arable soil types were used: a *Luvisol* with loamy sand texture and *Haplic Luvisol* with silt loam texture (same as in previous study, where more details on soil properties can be found (Lewicka-Szczebak et al., 2014)). The first part of these incubations (Exp 1.1) was performed for both soils at two different temperatures (8 and 22 °C) but with only one moisture level of 80 % WFPS (water filled pore space). The results of $\delta^{18}O(N_2O)$ analyses for these samples have already been published (Lewicka-Szczebak et al., 2014). Here we expand these data with $\Delta^{17}O(N_2O)$ analyses. The second part of static incubations

BGD
12, 17009–17049, 2015

(Exp 1.2) was performed for the same two soils but for three different moisture levels of 50, 65 and 80 % WFPS (target, for actual values see Table 1) at one temperature (22 °C).

This experimental approach is described in detail in Lewicka-Szczebak et al. (2014). In short, the soil was air dried and sieved at 2 mm mesh size. Afterwards, the soil was rewetted to obtain the target WFPS and fertilised with 50 (Exp 1.1) or 10 (Exp 1.2) mg N equivalents (as $NaNO_3$) per kg soil. The soils were thoroughly mixed to obtain a homogenous distribution of water and fertilizer and an equivalent of 100 g of dry soil was repacked into each incubation jar at bulk densities of 1.3 g cm^{-3} for the silt loam soil and 1.6 g cm^{-3} for the loamy sand soil. The 0.8 dm^3 Weck jars (J. WECK GmbH u. Co. KG, Wehr, Germany) were used with airtight rubber seals and with two three-way valves installed in their glass cover to enable sampling and flushing. The jars were flushed with N_2 at approximately 500 cm^3 min^{-1} (STP: 273.15 K, 100 kPa) for 10 min to create anoxic conditions. Immediately after flushing, acetylene (C_2H_2) was added to inhibit N_2O reduction in selected jars, by replacing 80 cm^3 of N_2 with C_2H_2, which resulted in 10 kPa C_2H_2 in the headspace. The soils were incubated for approximately 25 h and three to four samples were collected at 4 to 12 h-intervals by transferring 30 cm^3 of headspace gases into two pre-evacuated 12 cm^3 Exetainer vials (Labco Limited, Ceredigion, UK). The excess 3 cm^3 of headspace gas in each vial ensured that no ambient air entered the vials. The removed sample volume was immediately replaced by pure N_2 gas.

Additional treatments with addition of ^{15}N-labelled $NaNO_3$ (98 % ^{15}N isotopic purity) were used to control the efficiency of acetylene inhibition and to determine the N_2O mole fraction $f(N_2O) = c(N_2O)/[c(N_2) + c(N_2O)]$ (c: volumetric concentration) in non-inhibited treatments.

BGD
12, 17009–17049, 2015

2.1.2 Experiment 2 (Exp 2) – dynamic incubation under He atmosphere

The dynamic incubations were performed using a special gas-tight incubation system allowing for incubation under N_2-free atmosphere to enable direct quantification of soil N_2 fluxes (Butterbach-Bahl et al., 2002; Scholefield et al., 1997). This system has been described in detail by Eickenscheidt et al. (2014). Four different soils were incubated: two arable soils, same as in Exp 1 (loamy sand and silt loam) and two grassland soils: an organic soil classified as *Histic Gleysol* and a sandy soil classified as *Plaggic Anthrosol*. All soils were incubated at the target moisture level of 80 % WFPS and the two most active soils were additionally incubated at the lower moisture level of 70 % WFPS (target values, for actual values see Table 2).

The soils were air dried and sieved at 4 mm mesh size. Afterwards, the soil was rewetted to obtain 70 % WFPS and fertilised with 50 mg N equivalents (as $NaNO_3$) per kg soil. The soils were thoroughly mixed to obtain a homogenous distribution of water and fertilizer and 250 cm^3 of wet soil was repacked into each incubation vessel at bulk densities of 1.4 $g\,cm^{-3}$ for the silt loam soil, 1.6 $g\,cm^{-3}$ for the loamy sand soil, 1.5 $g\,cm^{-3}$ for the sandy soil, and 0.4 $g\,cm^{-3}$ for the organic soil. Afterwards the water deficit to the target WFPS was added on the top of the soil if needed. The incubation vessels were cooled to 2 °C and repeatedly evacuated (to 4.7 kPa) and flushed with He to reduce the N_2 background and afterwards flushed with a continuous flow of 20 % O_2 in helium (He/O_2) mixture at 15 $cm^3\,min^{-1}$ (STP) for at least 60 h. When a stable and low N_2 background (below 10 $\mu mol\,mol^{-1}$) was reached, temperature was increased to 22 °C. During the incubation the headspace was constantly flushed with He/O_2 mixture (first 3 days; Part 1) and then with He (last 2 days; Part 2) at a flow rate of approximately 15 $cm^3\,min^{-1}$ (STP). The fluxes of N_2O and N_2 were analyzed immediately (see Sect. 2.2). Samples for N_2O isotopocule analyses were collected by connecting the sampling vials in line with the exhaust gas of each incubation vessels and exchanging them at least twice a day. f (N_2O) was determined based on the direct measurement of N_2O and N_2 fluxes. The results presented in this study originate from the anoxic

BGD
12, 17009–17049, 2015

Part 2 of the incubation, since the N_2O fluxes during the Part 1 were too low for $\Delta^{17}O$ analyses. The results for two samples taken approximately 8 and 24 h after switch to anoxic conditions are shown.

2.2 Gas chromatographic analyses

In Exp 1 the samples for gas concentration analyses were collected in Exetainer vials (Labco Limited, Ceredigion, UK) and were analysed using an Agilent 7890A gas chromatograph (GC) (Agilent Technologies, Santa Clara, CA, USA) equipped with an electron capture detector (ECD). Measurement repeatability as given by the relative standard deviation (1σ) of four standard gas mixtures was typically 1.5 %.

In Exp 2, online trace gas concentration analysis of N_2 was performed with a micro-GC (Agilent Technologies, 3000 Micro GC), equipped with a thermal conductivity detector (TCD) and N_2O was measured with a GC (Shimadzu, Duisburg, Germany, GC–14B) equipped with ECD detector. The measurement repeatability (1σ) was better than 0.02 µmol mol^{-1} for N_2O and 0.2 µmol mol^{-1} for N_2.

2.3 Isotopic analyses

2.3.1 Isotopocules of N_2O

Gas samples were analyzed using a Delta V isotope ratio mass spectrometer (Thermo Scientific, Bremen, Germany) coupled to automatic preparation system: Precon + Trace GC Isolink (Thermo Scientific, Bremen, Germany) where N_2O was preconcentrated, separated and purified. In the mass spectrometer, N_2O isotopocule signatures were determined by measuring m/z 44, 45, and 46 of intact N_2O^+ ions as well as m/z 30 and 31 of NO^+ fragments ions. This allows the determination of average $\delta^{15}N^{av}$, $\delta^{15}N^{\alpha}$ ($\delta^{15}N$ of the central N position of the N_2O molecule), and $\delta^{18}O$ (Toyoda and Yoshida, 1999). $\delta^{15}N^{\beta}$ ($\delta^{15}N$ of the peripheral N position of the N_2O molecule) is calculated using $\delta^{15}N^{av} = (\delta^{15}N^{\alpha} + \delta^{15}N^{\beta})/2$. The ^{15}N site preference ($\delta^{15}N^{sp}$) is defined

BGD
12, 17009–17049, 2015

as $\delta^{15}N^{sp} = \delta^{15}N^{\alpha} - \delta^{15}N^{\beta}$. The scrambling factor and ^{17}O-correction were taken into account (Kaiser and Röckmann, 2008; Röckmann et al., 2003). Pure N_2O (Westfalen, Münster, Germany) was used as internal reference gas and was analyzed in the laboratory of the Tokyo Institute of Technology using calibration procedures reported previously (Toyoda and Yoshida, 1999; Westley et al., 2007). Moreover, the comparison materials from an intercalibration study (S1, S2) were used to perform a two-point calibration (Mohn et al., 2014).

All isotopic signatures are expressed as relative deviation from the $^{15}N/^{14}N$, $^{17}O/^{16}O$ and $^{18}O/^{16}O$ ratios of the reference materials (i.e., atmospheric N_2 and Vienna Standard Mean Ocean Water (VSMOW), respectively). The measurement repeatability (1σ) of the internal standard (filled into vials and measured in the same way as the samples) for measurements of $\delta^{15}N^{av}$, $\delta^{18}O$ and $\delta^{15}N^{sp}$ was typically 0.1, 0.1, and 0.5 ‰, respectively.

2.3.2 $\delta^{18}O$ of NO_3^-

Soil nitrate was extracted in 0.01 M aqueous $CaCl_2$ solution (weight ratio soil : solution 1 : 10) by shaking at room temperature for one hour. $\delta^{18}O$ of nitrate in the soil solution was determined using the bacterial denitrification method (Casciotti et al., 2002). The measurement repeatability (1σ) of the international standards (USGS34, USGS35, IAEA-NO-3) was typically 0.5 ‰ for $\delta^{18}O$.

2.3.3 $\Delta^{17}O$ excess in N_2O and NO_3^-

N_2O samples collected from soil incubation and N_2O produced from soil NO_3^- by the bacterial denitrifier method was analysed for $\Delta^{17}O$ using the thermal decomposition method (Kaiser et al., 2007) with a gold oven (Exp 1.1b, c and 1.2a, b) and with a gold-wire oven (Exp 1.1a and 2) (Dyckmans et al., 2015). The ^{17}O excess, $\Delta^{17}O$, is defined

BGD
12, 17009–17049, 2015

as (Kaiser et al., 2007):

$$\Delta^{17}O = \frac{1 + \delta^{17}O}{(1 + \delta^{18}O)^{0.5279}} - 1 \quad (1)$$

The measurement repeatability (1σ) of the international standards (USGS34, USGS35) was typically 0.5 ‰ for $\Delta^{17}O$.

2.3.4 Soil water analyses

Soil water was extracted with the method described by Königer et al. (2011) and $\delta^{18}O$ of water samples (with respect to VSMOW) was measured using cavity ringdown spectrometer Picarro L1115-*i* (Picarro Inc., Santa Clara, USA). The measurement repeatability (1σ) of the internal standards (three calibrated waters with known $\delta^{18}O$: −19.67, −8.60, +1.37 ‰) was below 0.1 ‰. The overall error associated with the soil water extraction method determined as standard deviation (1σ) of the 5 samples replicates was below 0.5 ‰.

2.4 Determination of the extent of isotope exchange

The extent of isotope exchange (x) was determined with two independent methods described below. In Exp 1 both approaches were applied simultaneously on the same soil samples, which allowed quantifying the oxygen isotope exchange with two different methods independently. This enabled the validation of the ^{17}O excess method, which was used here for the first time for quantification of isotope exchange. Afterwards this validated method was applied in the following Exp 2. For both presented methods it is assumed that no further O isotope exchange between N_2O and H_2O occurs.

2.4.1 $\delta^{18}O$ method

This method determines the isotope exchange based on the relative difference between $\delta^{18}O$ of produced N_2O and its potential precursors: soil water and soil nitrate

BGD
12, 17009–17049, 2015

(Snider et al., 2009). To make this method applicable, parallel incubations with distinct water and/or nitrate isotopic signatures must be carried out. In Exp 1 this was achieved by rewetting the soils with two different waters of distinct isotopic signatures: *heavy water* ($\delta^{18}O = -1.5$ ‰) and *light water* ($\delta^{18}O = -14.8$ ‰) and by adding two different nitrate fertilizers: natural *Chile saltpeter* ($NaNO_3$, Chili Borium Plus, Prills-Natural origin, supplied by Yara, Dülmen, Germany, $\delta^{18}O = 56$ ‰) and *synthetic NaNO*$_3$ (Sigma Aldrich, Taufkirchen, Germany, $\delta^{18}O = 27$ ‰).

The calculation is based on two end member mixing model (water (δ_w) and nitrate (δ_n); δ stands for $\delta^{18}O(N_2O)$) taking into account the isotope fractionation associated with O incorporation into N_2O from each end member (ε_w – fractionation associated with oxygen isotope exchange with water, ε_n – fractionation associated with branching effect during nitrate reduction). This is expressed as:

$$1 + \delta = x(1 + \delta_w)(1 + \varepsilon_w) + (1 - x)(1 + \delta_n)(1 + \varepsilon_n) \quad (2)$$

which can be rearranged to:

$$\frac{\delta - \delta_n}{1 + \delta_n} = x(1 + \varepsilon_w)\frac{\delta_w - \delta_n}{1 + \delta_n} + x\varepsilon_w + (1 - x)\varepsilon_n \quad (3)$$

where:

$\frac{\delta - \delta_n}{1 + \delta_n} = \delta^{18}O(N_2O/NO_3^-)$ = dependent variable of the linear regression,

$\frac{\delta_w - \delta_n}{1 + \delta_n} = \delta^{18}O(H_2O/NO_3^-)$ = independent variable of the linear regression,

$x(1 + \varepsilon_w)$ = slope of the linear regression ≅ the magnitude of isotope exchange (x),

$x\varepsilon_w + (1 - x)\varepsilon_n$ = intercept of the linear regression ≅ total fractionation (ε).

Hence, from the linear correlation between $\delta^{18}O(N_2O/NO_3^-)$ and $\delta^{18}O(H_2O/NO_3^-)$ we can read approximate x (the deviation from the exact value may be up to 0.02, for $\varepsilon_w < 20$ ‰) and the total fractionation ε comprised of both ε_w and ε_n.

BGD
12, 17009–17049, 2015

2.4.2 $\Delta^{17}O$ method

This method determines the isotope exchange based on the comparison of $\Delta^{17}O$ in soil nitrate and produced N_2O. It requires the application of nitrate characterised by high $\Delta^{17}O$. In Exps 1 and 2 soils were amended with natural $NaNO_3$ Chile saltpeter showing high $\Delta^{17}O$ (ca. 20 ‰) and with synthetic $NaNO_3$ showing slight negative $\Delta^{17}O$ (ca. −5 ‰) and the $\Delta^{17}O$ of the N_2O product was measured. $\Delta^{17}O$ of soil water was assumed 0 ‰.

The magnitude of oxygen isotope exchange (x) was calculated as:

$$x = 1 - \frac{\Delta^{17}O(N_2O)}{\Delta^{17}O(NO_3^-)} \quad (4)$$

The error due to the use of the power-law definition of $\Delta^{17}O$ in combination with a linear mixing relationship (Eq. 4) causes a negligible relative bias of < 1 % for x.

2.5 Correction for N_2O reduction

Since $\delta^{18}O(N_2O)$ values of emitted N_2O are strongly affected by partial N_2O reduction, the measured isotope values can only be informative for the mechanism of N_2O production if the reduction is inhibited or the isotope effects associated with reduction are taken into account. In Exp 1.2 N_2O reduction was completely inhibited, whereas in Exp 1.1 we had treatments with and without inhibition. Exp 1.1 thus allows us to check the validity of our correction methods as it directly yields the impact of N_2O reduction on the measured $\delta^{18}O(N_2O)$ values. In Exp 2, reduction was not inhibited and the mathematical correction described below was applied.

The correction was made using the Rayleigh fractionation equation (Mariotti et al., 1981):

$$\frac{1+\delta_S}{1+\delta_{S0}} = f^{\varepsilon} \quad (5)$$

BGD
12, 17009–17049, 2015

where: δ_S – isotopic signature of the remaining substrate, here: measured $\delta^{18}O$ of the final, partially reduced, N_2O, δ_{S0} – initial isotopic signature of the substrate, here: $\delta^{18}O$ of the produced N_2O unaffected by the reduction ($\delta_0^{18}O$); to be calculated; f – remaining unreacted fraction, here: the N_2O mole fraction f (N_2O); directly measured; ε – isotope effect between product and substrate, here: ε (N_2/N_2O), the isotope effect associated with N_2O reduction, taken from the literature (Lewicka-Szczebak et al., 2014). As it has been shown that the experimental approach largely influences O isotope effect during reduction (Lewicka-Szczebak et al., 2014, 2015), we used different $\varepsilon^{18}O(N_2/N_2O)$ values for static and dynamic conditions. For the static Exp 1 a mean $\varepsilon^{18}O(N_2/N_2O)$ value of −17.4 ‰ is used, based on one common experiment between the study of Lewicka-Szczebak et al. (2014) (Experiment 1) and this study (Exp 1.1). For the dynamic Exp 2 we accept the $\varepsilon^{18}O(N_2/N_2O)$ value of −12 ‰ recently determined for a dynamic experiments under He/O_2 atmosphere (Lewicka-Szczebak et al., 2015). For the correction of $\delta^{15}N^{sp}$ values one common $\varepsilon^{15}N^{sp}$ (N_2/N_2O) value of −5 ‰ was used, since it was shown that this value is applicable for all experimental setups (Lewicka-Szczebak et al., 2014). The error due to the simplified use of $\varepsilon^{15}N^{sp}$ for the Rayleigh model (Eq. 5) instead of separate calculations with $\varepsilon^{15}N^{\alpha}$ and $\varepsilon^{15}N^{\beta}$, causes a negligible bias of the calculated $\delta_0^{15}N^{sp}$ values of < 0.15 ‰ for the presented dataset.

2.6 Statistical methods

For results comparisons, ANOVA variance analysis was used with the significance level α of 0.05. The uncertainty values provided for the measured parameters represent the standard deviation (1σ) of the replicates. The propagated uncertainty was calculated using Gauss' error propagation equation taking into account standard deviations of all individual parameters.

BGD
12, 17009–17049, 2015

3 Results

3.1 Exp 1

In Table 1 the results are presented as average values from three replicated incubation vessels with respective standard deviation. Soil nitrate and water were analysed at the beginning of the experiment from the prepared homogenised soils, hence no standard deviation but the standard analytical uncertainty is given. Relative isotope ratio differences between N_2O and soil water, $\delta^{18}O(N_2O/H_2O)$, were calculated as the difference between the measured $\delta^{18}O$ in produced N_2O and soil water:

$$\delta^{18}O(N_2O/H_2O) = \frac{\delta^{18}O(N_2O) - \delta^{18}O(H_2O)}{1 + \delta^{18}O(H_2O)} \quad (6)$$

In samples where N_2O reduction occurred these values were corrected as described above (Sect. 2.5) and for statistical analyses and modelling exercises the reduction-corrected values were used ($\delta_0^{18}O(N_2O/H_2O)$).

For different temperature treatments, x was not significantly different ($p = 0.19$) but $\delta^{18}O(N_2O/H_2O)$ was slightly higher ($p = 0.009$) for 8 °C ((19.5 ± 0.3) ‰) than for 22 °C ((18.6 ± 0.3) ‰) treatment. No significant differences were observed between the two analysed soil types or between various soil moisture levels.

When comparing Exp 1.1 and 1.2, x did not show any significant differences, but the $\delta_0^{18}O(N_2O/H_2O)$ values were significantly different ($p < 0.001$) with higher values for Exp 1.1 ((19.1 ± 0.5) ‰) than for Exp 1.2 ((16.9 ± 0.8) ‰). It should be noted that the $\delta^{18}O$ values of soil nitrate were much lower in Exp 1.2 (from −2.0 to 6.5 ‰) when compared to Exp 1.1 (from 31.8 to 42.6 ‰) which might have affected the observed differences in $\delta^{18}O(N_2O/H_2O)$.

BGD
12, 17009–17049, 2015

3.2 Exp 2

In Table 2 the results are presented as average values from three replicate incubation vessels with respective standard deviation. The extent of oxygen isotope exchange (x) ranges from 55 to 85 % and is lower and much more variable when compared to Exps 1.1 and 1.2. $\delta_0^{18}O(N_2O/H_2O)$ varies between 18.6 and 36.9 ‰, which is significantly higher when compared to the values determined in Exp 1.

4 Discussion

4.1 Determination of oxygen isotope exchange

For Exp 1 the $\delta^{18}O$ method was applied to estimate x and ε from the relationship between $\delta^{18}O(N_2O/NO_3)$ and $\delta^{18}O(H_2O/NO_3)$ as described in Sect. 2.4.1.

According to this method, from the linear regression one can decipher x (slope) and ε (intercept) (Snider et al., 2009). The correlation is excellent (R^2 from 0.989 to 0.997) which indicates that the x and ε are very stable for all the treatments (Fig. 2). The x is about 1 (complete exchange) and ε varies from 17.1 (Exp 1.2) to 18.2 ‰ (Exp 1.1). When compared to the results presented in Table 1, we see slightly higher isotope exchange with $\delta^{18}O$ method when compared to $\Delta^{17}O$ method. This may be partially due to the fact that the slope in $\delta^{18}O$ method (Fig. 2) is actually slightly higher than x (from Eq. 3: $x(1+\varepsilon_w)$). But the difference between the two experiments is mostly within the error of each method, so far the results are consistent. The $\Delta^{17}O$ method is more useful, since it allows for individual determinations of x, whereas the correlation obtained from the $\delta^{18}O$ method is based on all data, hence provides a mean result for x and ε for a whole experiment.

Importantly, we found that the $\delta^{18}O$ method is not applicable for samples with uninhibited N_2O reduction, if $\delta^{18}O(N_2O)$ values are not corrected for N_2O reduction. The treatment with uninhibited reduction of Exp 1.1 was tested and provided very differ-

BGD
12, 17009–17049, 2015

ent results, i.e. largely overestimated x (1.5) and ε (44.8) (red dashed fit line, Fig. 2). Hence, for proper determination of these factors the results from treatments with inhibited N_2O reduction were used (solid black fit line, Fig. 2). However, the $\delta^{18}O$ values after mathematical correction for N_2O reduction (red "+" points, Fig. 2) fitted very well to the correlation found for inhibited samples. Hence, the reduction corrected values ($\delta_0^{18}O(N_2O)$) should rather be used when applying this method in experiments with uninhibited N_2O reduction. Moreover, in both static experiments we used C_2H_2 inhibition technique, and our results indicate almost complete exchange of oxygen isotopes with soil water, which indicates clearly that the isotope exchange process is not inhibited by C_2H_2 addition.

4.2 Oxygen isotope effects at nearly complete isotope exchange

In case of very high, almost complete, isotope exchange with soil water (Exp 1), the relative isotope ratio difference between N_2O and H_2O ($\delta_0^{18}O(N_2O/H_2O)$) is quite stable and ranges from 15.6 to 19.8 ‰ (Table 1). In contrast, the relative isotope ratio difference between N_2O and NO_3^- ($\delta_0^{18}O(N_2O/NO_3^-)$) shows large variations from −36.1 to 18.0 ‰ (Fig. 3).

ε determined in Fig. 2 represents theoretically the total oxygen isotope fractionation (from Eq. 3: $x\varepsilon_w + (1-x)\varepsilon_n$), but in case of the nearly whole isotope exchange ($x = 1$) ε equals ε_w and $\varepsilon_w = (\delta_{N_2O} - \delta_w)/(\delta_w + 1) = \delta^{18}O(N_2O/H_2O)$, hence both – the intercept in Fig. 2 and $\delta^{18}O(N_2O/H_2O)$ in Fig. 3 should provide rough estimates for ε_w. However, for $x < 1$ $\delta^{18}O(N_2O/H_2O)$ depends also on δ_n and ε_n and the intercept (Fig. 2) includes ε_n. Both these values indicate a slight difference between both experiments, for Exp 1.1 ε of (18.2 ± 0.6) (Fig. 2) and $\delta^{18}O(N_2O/H_2O)$ of (19.1 ± 0.5) (Table 1) are higher than for Exp 1.2, (17.1 ± 0.3) and (16.7 ± 0.8), respectively. This slight difference is most probably due to x slightly lower than 1, as indicated by $\Delta^{17}O$ method and additional impact of δ_n and ε_n. It can be noted that $\delta_0^{18}O(N_2O/H_2O)$ slightly increases with higher $\delta^{18}O$ values of nitrate (Fig. 3), i.e. the difference of about 40 ‰ in $\delta^{18}O$ of applied

BGD
12, 17009–17049, 2015

NO_3^- results in about 2‰ change in $\delta_0^{18}O(N_2O/H_2O)$. Hence, only about 5 % of the difference in nitrate isotopic signature is reflected in the produced N_2O, suggesting that an equivalent percentage of $O(N_2O)$ originated from NO_3^-. This is very consistent with the determined extent of isotope exchange with soil water, which was (95.6±2.6) % (Table 1).

Taken together, the data indicates that the $\delta^{18}O(N_2O)$ values are clearly influenced by the $\delta^{18}O$ of soil water, whereas $\delta^{18}O$ of soil nitrates has only very little influence. Hence, the O isotope fractionation during N_2O production by denitrification should be considered in relation to soil water, rather than soil nitrates.

4.3 Oxygen isotope effects at variable isotope exchange

In contrast to the above presented results, for the dynamic incubation (Exp 2), x was more variable and significantly lower. In general, the lower x was associated with higher $\delta_0^{18}O(N_2O/H_2O)$ values. In Fig. 4 we can compare results from static incubations (red symbols) with the dynamic incubations (black symbols). This comparison clearly shows that the pattern of isotope exchange and the associated oxygen fractionation differs significantly between both experimental approaches. The essential difference in Exp 2 was the use of a flow-through system and of oxic atmosphere at the beginning of the incubation (though results presented originate from the anoxic phase). This resulted in lower production rates for N_2O when comparing the respective soil (Tables 1 and 2), e.g., 80 $\mu g\,kg^{-1}\,h^{-1}$ (mass of N as sum of N_2O and N_2 per mass of dry soil) for the silt loam soil at 80 % WFPS in Exp 2.3 but 261 $\mu g\,kg^{-1}\,h^{-1}$ in Exp 1.1c. This may suggest an impact of N_2O production rate on extent of isotope exchange. However, for static experiments the effect of production rate was not observed, e.g. between 1.1a and 1.1b (Table 1), where we have different production rates but similar x and $\delta_0^{18}O(N_2O/H_2O)$. Hence, we rather suppose that the trend observed here may be due to activity of different microorganism groups, which have been activated by oxic atmosphere in Exp 2 and are characterised by lower x and higher $\delta_0^{18}O(N_2O/H_2O)$.

BGD
12, 17009–17049, 2015

Interestingly, the correlation between x and $\delta_0^{18}O(N_2O/H_2O)$ seems to differ for different soil types. Very clearly both sandy soils represent distinct and weaker correlation when compared to silt loam and organic soil. Most probably this is due to different oxygen fractionation pattern in both soils, which we try to decipher in the theoretical model presented below.

4.4 The mechanism of oxygen isotope fractionation – a fractionation model

To better understand the mechanism of oxygen isotope fractionation and the relation between the apparent isotope effect and the extent of isotope exchange we applied a simulation calculation where the total isotope effect was calculated from the theoretical isotope fractionation associated with two enzymatic reduction steps: NIR and NOR. This model was based on the calculations presented by Rohe et al. (2014a) for pure fungal cultures, where this approach has been described in detail. The model assumes that $\delta^{18}O(N_2O)$ is determined by two isotope fractionation processes associated (i) with the branching isotope effect (ε_n) and (ii) with the isotope effect due to isotope exchange with soil water (ε_w), both possible at NIR or NOR. This can be expressed by the following isotope mass balance equations:

$$1 + \delta = x_{NOR}(1 + \delta_w)(1 + \varepsilon_w) + (1 - x_{NOR})(1 + \delta_{NO})(1 + \varepsilon_{NOR}) \quad (7)$$

$$1 + \delta_{NO} = x_{NIR}(1 + \delta_w)(1 + \varepsilon_w) + (1 - x_{NIR})(1 + \delta_n)(1 + \varepsilon_{NIR}) \quad (8)$$

where:

$$1 - x = (1 - x_{NIR})(1 - x_{NOR}) \quad (9)$$

$$1 + \varepsilon_n = (1 + \varepsilon_{NIR})(1 + \varepsilon_{NOR}) \quad (10)$$

After substitution and transformation, this gives

$$\frac{\delta - \delta_w}{1 + \delta_w} = (1 - x)(1 + \varepsilon_n)\frac{\delta_n - \delta_w}{1 + \delta_w} + (x - x_{NOR})\varepsilon_{NOR}(1 + \varepsilon_w) + x\varepsilon_w + (1 - x)\varepsilon_n \quad (11)$$

BGD
12, 17009–17049, 2015

We have neglected the possible fractionation associated with the NAR reduction, i.e. $\delta(NO_2^-) = \delta(NO_3^-) = \delta_n$ in Eq. (11). This enzymatic step was investigated by Rohe et al. (2014a), and appeared to have very minor impact on the total oxygen fractionation, i.e. this step was relevant only for one fungus species. Hence, we only focused here on differentiating between NIR and NOR enzymatic reduction steps, which are most likely the enzymatic reactions crucial for determining final N_2O isotopic values (Kool et al., 2007).

There are a lot of unknown factors in the Eq. (11); first of all, isotopic fractionation factors ε_n and ε_w. We have compiled the results of both methods applied for Exp 1 data: $\delta^{18}O$ method and $\Delta^{17}O$ method to estimate these factors. Using $\delta^{18}O$ method ε was determined from the intercept in Fig. 2 and this value represents total fractionation: $\varepsilon = x\varepsilon_w + (1-x)\varepsilon_n$ (see Sect. 2.4.1). Using $\Delta^{17}O$ method the individual x was calculated for each sample. We have also measured $\delta^{18}O(N_2O/H_2O)$ and $\delta^{18}O(NO_3^-/H_2O)$ for each sample, hence from the transformed Eq. (3):

$$\frac{\delta - \delta_w}{1 + \delta_w} = (1 - x)(1 + \varepsilon_n)\frac{\delta_n - \delta_w}{1 + \delta_w} + x\varepsilon_w + (1 - x)\varepsilon_n \quad (12)$$

and knowing that $x\varepsilon_w + (1-x)\varepsilon_n = 0.0181$ for Exp 1.1 and $x\varepsilon_w + (1-x)\varepsilon_n = 0.0172$ for Exp 1.2 (Fig. 2) we have calculated ε_w and ε_n for each sample. Table 3 summarises the results.

The determination of ε_w is very precise, with no significant difference between Exp 1.1 and 1.2 ($p = 0.868$). The value obtained (17.5 ± 0.7) ‰ is within the range of the previous values determined for chemical exchange ε $(NO_2^-/H_2O) = 14$ ‰ and ε $(NO_3^-/H_2O) = 23$ ‰ (Böhlke et al., 2003; Casciotti et al., 2007). So far there are no data for isotope effect of chemical exchange ε (NO/H_2O). The ε_w value determined here is a hypothetical mean value of enzymatically mediated isotope exchange associated with NIR (ε_w (NO_2^-/H_2O)) and NOR (ε_w (NO/H_2O)).

ε_n is also quite stable with a weak ($p = 0.006$) and very small (below 1 ‰) difference between Exp 1.1 and 1.2. The ε_n values found are very low and vary around 0, from

BGD
12, 17009–17049, 2015

−1.9 to 2.1 ‰. This is much lower compared to previous studies which reported ε_n from 10 to 30 ‰ (Casciotti et al., 2007; Rohe et al., 2014a).

We checked how well these calculated values fit for the individual samples of both experiments. We started with the simplest Scenario 0, where we assume the values determined in Table 3 for ε_w and ε_n and calculate the $\delta^{18}O(N_2O)$ with Eq. (11), which is then compared with the measured $\delta^{18}O(N_2O)$ and the difference between measured and calculated $\delta^{18}O(N_2O)$ value (D) is determined (Table 4). Since the mean value of 0 was assumed for ε_n in this scenario, the isotope exchange can be associated either with NIR or NOR without any effect on the final $\delta^{18}O(N_2O)$, because the Eq. (11) is simplified to:

$$\frac{\delta - \delta_w}{1 + \delta_w} = (1 - x)\frac{\delta_n - \delta_w}{1 + \delta_w} + x\varepsilon_w \quad (13)$$

This scenario works quite well for Exp 1 data with the maximal D of 1.4 ‰. However, for Exp 2 data we obtain significant overestimation of the calculated $\delta^{18}O(N_2O)$ values for sandy soils (Exp 2.1 and 2.2) up to 6.1 ‰ and underestimation for two other soils, reaching up to 12.2 ‰ for organic soil (Exp 2.5). Why the model developed based on Exp 1 data do not work for Exp 2 data? We expect that the ε_w value should be quite stable for all the samples. It was observed in the study by Casciotti et al. (2007) that ε (NO_2^-/H_2O) values varied in a very narrow range. Also in our study in Fig. 2 we obtained very good correlation with stable slope which suggests that the ε_w value must be very stable and almost identical for all the samples. It can be supposed that rather ε_n values can be more variable, but due to nearly complete isotope exchange in Exp 1 these potential variations cannot be reflected in $\delta^{18}O(N_2O)$ values. Also, the previous study by Rohe et al. (2014a) indicated possibly wide variations of ε_n from 10 to 30 ‰.

Therefore, for the next scenarios (Scenario 1, 2 and 3 – Table 4) we assumed stable ε_w value of 17.5 ‰, as determined from Exp 1 (Table 3) and ε_n values were calculated individually for each sample with Eq. (11) from the $\delta_0^{18}O(N_2O/H_2O)$ values. In each scenario ε_n was equally distributed between NIR and NOR according to Eq. (10),

BGD
12, 17009–17049, 2015

so that $\varepsilon_{NIR} = \varepsilon_{NOR}$. For our samples we know the value of total isotope exchange (x determined with $\Delta^{17}O$ method), but we do not know at which enzymatic step(s) this exchange occurred. Since the isotope exchange has very different impact on the final $\delta^{18}O(N_2O)$ when associated with NIR or NOR, we can obtain this information by comparing different scenarios (Table 4). In Scenario 1 the total isotope exchange is associated with the first reduction step NIR and in Scenario 2, with the final reduction step NOR. In Scenario 3 the total isotope exchange is equally distributed between both steps NIR and NOR according to Eq. (9) so that $x_{NIR} = x_{NOR}$. Actually, in this study we cannot precisely determine the enzymatic step where the isotope exchange occurs, but rather the relative relation between the both isotope effects. Namely, in Scenario 1 the exchange effect associated with x_{NIR} precedes the branching effect at NOR (ε_{NOR}) and, conversely, in Scenario 2 the exchange isotope effect associated with x_{NOR} occurs later than the both branching effects (ε_{NIR}, ε_{NOR}). Hence, in Scenario 1 the ε_{NOR} has more direct impact on the final $\delta^{18}O(N_2O)$ whereas in Scenario 2 the last fractionation step is due to ε_w (Eq. 11). Therefore, applying different scenarios results in different values of calculated ε_n (Table 4).

The narrowest range of variations of the calculated ε_n values was obtained in Scenario 1. For Exp 1 they vary around 0, similarly to the results presented in Table 3, which indicates that this model and the equations applied for $\delta^{18}O$ method (Eq. 12) are actually the same. For Exp 2 the calculated ε_n values are negative for sandy soils (Exp 2.1 and 2.2) from −9.1 to −6.2 ‰ and positive for other soils with lower values for silt loam from 1.6 to 3.8 ‰ and higher for organic soil from 3.8 to 18.1 ‰ (Table 4). Variations of calculated ε_n values are much larger in Scenario 2 with especially very wide range for Exp 1 from −72.8 to +38.5 ‰. For Exp. 2 similar trend as in Scenario 1 is observed, with negative values for sandy soils (down to −20.0 ‰) and highest values for organic soil (up to 37.1 ‰). The absolute values are generally larger and the variations among them are thereby increased when compared to Scenario 1. The strongly negative ε_n values obtained in Scenario 2 are rather out of the plausible range of values. Moreover, for the last sample of Exp 1 where $x = 1$ this scenario fails in finding

BGD
12, 17009–17049, 2015

the ε_n value for $D = 0$, because for the complete isotope exchange at x_{NOR} branching effect has no impact on the final $\delta^{18}O(N_2O)$. However, the residual $D = 0.2$ ‰ is very low, which do not exclude this scenario. But still Scenario 1 is more plausible because (i) the overall ε_n variations are smaller and (ii) we do not find extremely negative values. Results from Scenario 3 are situated in the middle of Scenario 1 and 2, and show larger variations than Scenario 1, but without the extreme outliers, hence can be also a plausible model. From comparison of these scenarios we can say that the isotope exchange is definitely associated with NIR and may also take place at both steps but not solely at NOR. This reinforces the previous findings from pure culture studies which suggested the majority of isotope exchange associated mainly with nitrite reduction (Garber and Hollocher, 1982; Rohe et al., 2014a).

For each scenario our model indicated rather lower ε_n values than previously assumed (Casciotti et al., 2007; Rohe et al., 2014a). But actually, the isotope effect determined by Casciotti et al. (2007), +25 to +30 ‰, takes only the intra-molecular branching effect into account, because in the bacterial denitrification method the whole nitrate pool is quantitatively consumed, hence the inter-molecular isotope effect cannot manifest. Therefore, the values found by Casciotti et al. (2007) represent the maximal possible branching effect. In the experiment presented by Rohe et al. (2014a) only very little of added substrate was reduced, hence we should also observe the inter-molecular effects. Indeed, the values for ε_{NIR} were lower down to +10 ‰ and ε_{NAR} was assumed 0 ‰. This may suggest that the net branching effect decreases with smaller reaction rates because of inter-molecular isotope fractionation. But are the negative net branching effects actually possible? It could be the case only if the inter-molecular effect exceeds the intra-molecular effect, i.e. the former must be more negative than −30 ‰. An idea about the magnitude of the intra-molecular effect can be obtained from the change in isotopic signature of the remaining nitrate, since this reflects the enrichment in residual nitrate-^{18}O due to intra-molecular effects. In pure culture studies this effect ranges from −23 to −5 ‰ (Granger et al., 2008), but in soil incubations values as low as −37 ‰ have been observed (Exp. 1F in Lewicka-Szczebak et al., 2014). Hence,

BGD
12, 17009–17049, 2015

slightly negative net ε_n is theoretically possible, but up to a few ‰ for each enzymatic step, which gives the minimal ε_n of about −10 ‰. Therefore, the results of Scenario 2 must be rejected, whereas the values found in Scenario 1 are most plausible.

4.5 Significance for quantification and differentiation of soil denitrification

From the presented results it is most surprising and incomprehensible, why the same soils show various extents of isotope exchange with soil water, and especially, why this exchange was high and stable in static experiment and decreases by dynamic incubations. Most probably, in the static inhibited experiments denitrification is the only N_2O producing process and in the dynamic uninhibited incubations other N_2O producing processes may significantly contribute to N_2O production. These incubations were performed initially under oxic conditions, which were switched to anoxic conditions after three days. However, all the results presented here originate from this anoxic phase, since the N_2O production during oxic phase was too low for $\Delta^{17}O$ analyses. Hence, the potentially contributing processes might be fungal denitrification, co-denitrification, nitrifier denitrification or dissimilatory nitrate reduction to ammonium (DNRA). ^{15}N site preference ($\delta^{15}N^{sp}$) may be used as a tracer to distinguish some of these processes. It is known that fungal denitrification and nitrification are characterized by significantly higher $\delta^{15}N^{sp}$ values (33 to 37 ‰, Rohe et al., 2014a; Sutka et al., 2008, 2006) when compared to bacterial denitrification and nitrifier denitrification (−11 to 0 ‰, Sutka et al., 2006; Toyoda et al., 2005). To check the hypothesis of mixing of N_2O from various sources we plotted $\delta_0^{18}O$ (N_2O/H_2O) values against $\delta_0^{15}N^{sp}$ values of produced N_2O (Fig. 5).

It can be clearly noticed that the results from the inhibited experiment (Exp 1, red symbols) fit perfectly into the field of bacterial denitrification. Similarly, the results of sandy soils from the Exp 2 show a slightly wider range, but still are typical for bacterial denitrification. In contrast, silt loam soil (Exp 2.3, 2.4) and the organic soil (Exp 2.5, 2.6) both show increased $\delta_0^{18}O(N_2O/H_2O)$ and $\delta_0^{15}N^{sp}$ values which are very well cor-

BGD
12, 17009–17049, 2015

related. This could indicate that in Exp 2 another process characterized by high $\delta^{15}N^{sp}$ and $\delta^{18}O$ values has significant contribution to total N_2O production by these two soils. This could be nitrification, which is rather not plausible due to the anoxic conditions, or fungal denitrification. But it remains unclear why this was not observed in the inhibited static experiment for the same soil (silt loam). C_2H_2 inhibition do not affect fungal denitrification (Maeda et al., 2015) as far as NO_3^- and NO_2^- availability is not restricted by inhibited nitrification. However, in the dynamic experiments, the first oxic phase might have activated other microorganisms, possibly preferentially fungi. This could explain that their contribution is observed only in Exp 2 but not in Exp 1. Such an activation of denitrification by oxygen supply has been documented for one fungus species (Zhou et al., 2001).

We verified if the correlation presented in Fig. 5 could have resulted from calculation artefacts, since all of the higher $\delta_0^{18}O(N_2O/H_2O)$ and $\delta_0^{15}N^{sp}$ values were corrected for N_2O reduction (according to the method described in Sect. 2.5). This correction method does not provide very precise results, since the isotope effects associated with N_2O reduction are not entirely stable and predictable (Lewicka-Szczebak et al., 2015; Lewicka-Szczebak et al., 2014). Therefore we have checked if this correlation may be only a calculation artifact and recalculated the values assuming larger range of isotopic fractionations (±5 ‰, resulting in $\varepsilon^{15}N^{sp}$ (N_2/N_2O) from −10 to 0 ‰ and $\varepsilon^{18}O(N_2/N_2O)$ from −20 to −6 ‰). Results show that the correlation may slightly change in slope (from 0.41 to 0.85), intercept (from −10.4 to −18.0) and significance (R^2 from 0.64 to 0.91). But it always keeps the same trend, i.e. for the Exps 2.3–2.6 we obtain in any case correlated increase of $\delta_0^{15}N^{sp}$ and $\delta_0^{18}O$ (N_2O/H_2O) (see grey dashed lines in Fig. 5), proving that the indication for further contributing processes cannot be an artefact of the correction approach. For these experiments (2.3–2.6) in our model calculations (Table 4) always higher ε_n values were found when compared to Exp 1 and 2.1–2.2. Also for pure culture studies of fungal denitrification the ε_n values determined by a similar modelling approach were higher, up to 30 ‰ (Rohe et al., 2014a). This would support the hypothesis on fungal denitrification contribution.

BGD
12, 17009–17049, 2015

4.6 Source of $\Delta^{17}O$ in atmospheric N_2O

In Exp 1 the $\Delta^{17}O(N_2O)$ values obtained from all measured N_2O samples were very low. Moreover, we also included the treatment with chemical nitrate as fertilizer, characterised by negative $\Delta^{17}O$ excess, and the produced N_2O did not show any positive $\Delta^{17}O$ excess (Table 1). The produced N_2O is always characterised by smaller ^{17}O-excess ($\Delta^{17}O$ values closer to 0) than in the source nitrate (Table 1). These results indicate that denitrification produces N_2O of randomly distributed oxygen, due to mostly very high extent of isotope exchange with soil water and the consequent loss of ^{17}O excess of nitrate. However, in Exp 2 numerous samples showed lower extent of isotope exchange, down to 50 %, and the ^{17}O excess of nitrate is partially transferred to N_2O, resulting in $\Delta^{17}O(N_2O)$ up to 5 ‰. This indicates that denitrification may be potentially the source of atmospheric N_2O with ^{17}O excess, as previously supposed (Kaiser et al., 2004; Michalski et al., 2003), but the magnitude of this excess is largely reduced by the exchange of oxygen isotopes with randomly distributed soil water.

5 Conclusions

It can be supposed that bacterial denitrification in soils is characterised by quite stable $\delta_0^{18}O(N_2O/H_2O)$ of 17.5 ± 1.2 ‰ due to the nearly complete O isotope exchange and constant isotope effect associated with this exchange. Hence, when N_2O producing processes other than heterotrophic processes are negligible, $\delta_0^{18}O(N_2O)$ can be well predicted. Conversely, $\delta_0^{18}O(N_2O/H_2O)$ values larger than 19 ‰ are probably indicative for the contribution of other processes. But more work on oxygen isotope effects during N_2O production of those other processes is needed to obtain robust estimate of their contribution. It is necessary to conduct experiments to determine the possible range of $\delta_0^{18}O(N_2O/H_2O)$ for other N_2O producing processes. From the studies available until now, we can make a first estimate for $\delta_0^{18}O(N_2O/H_2O)$ characteristic

BGD
12, 17009–17049, 2015

of fungal denitrification of 48.2 ± 3.7 ‰ (when disregarding two most extreme values; for all results 47.4 ± 10.3 ‰) (Rohe et al., 2014a). This value is very different from the $\delta_0^{18}O(N_2O/H_2O)$ of bacterial denitrification determined here (17.5±1.2 ‰) which opens a new perspective of applying $\delta_0^{18}O(N_2O/H_2O)$ for differentiation between fungal and bacterial denitrification.

Acknowledgements. This study was supported by German Research Foundation (DFG We/1904-4). Many thanks are due to Anette Giesemann and Martina Heuer for help in N_2O isotopic analyses; Lars Szwec for $\Delta^{17}O$ analyses; Kerstin Gilke for help in chromatographic analyses, Caroline Buchen for supplying soil for laboratory incubations and Maciej Lewicki for supplying the isotopically depleted water from the Tatra Mountains, Poland.

References

Böhlke, J. K., Mroczkowski, S. J., and Coplen, T. B.: Oxygen isotopes in nitrate: new reference materials for O-18: O-17: O-16 measurements and observations on nitrate-water equilibration, Rapid Commun. Mass. Sp., 17, 1835–1846, 2003.

Butterbach-Bahl, K., Willibald, G., and Papen, H.: Soil core method for direct simultaneous determination of N-2 and N_2O emissions from forest soils, Plant Soil, 240, 105–116, 2002.

Casciotti, K. L., Bohlke, J. K., McIlvin, M. R., Mroczkowski, S. J., and Hannon, J. E.: Oxygen isotopes in nitrite: analysis, calibration, and equilibration, Anal. Chem., 79, 2427–2436, 2007.

Casciotti, K. L., Sigman, D. M., Hastings, M. G., Bohlke, J. K., and Hilkert, A.: Measurement of the oxygen isotopic composition of nitrate in seawater and freshwater using the denitrifier method, Anal. Chem., 74, 4905–4912, 2002.

Dyckmans, J., Lewicka-Szczebak, D., Szwec, L., Langel, R., and Well, R.: Comparison of methods to determine triple oxygen isotope composition, Rapid Commun. Mass. Sp., 29, 1991–1996, 2015.

Eickenscheidt, T., Heinichen, J., Augustin, J., Freibauer, A., and Drösler, M.: Nitrogen mineralization and gaseous nitrogen losses from waterlogged and drained organic soils in a black alder (*Alnus glutinosa* (L.) Gaertn.) forest, Biogeosciences, 11, 2961–2976, doi:10.5194/bg-11-2961-2014, 2014.

BGD
12, 17009–17049, 2015

Garber, E. A. E. and Hollocher, T. C.: N-15, O-18 tracer studies on the activation of nitrite by denitrifying bacteria – nitrite water–oxygen exchange and nitrosation reactions as indicators of electrophilic catalysis, J. Biol. Chem., 257, 8091–8097, 1982.

Granger, J., Sigman, D. M., Lehmann, M. F., and Tortell, P. D.: Nitrogen and oxygen isotope fractionation during dissimilatory nitrate reduction by denitrifying bacteria, Limnol. Oceanogr., 53, 2533–2545, 2008.

Kaiser, J. and Röckmann, T.: Correction of mass-spectrometric isotope ratio measurements for isobaric isotopologues of O_2, CO, CO_2, N_2O and SO_2, Rapid Commun. Mass Sp., 22, 3997–4008, 2008.

Kaiser, J., Rockmann, T., and Brenninkmeijer, C. A. M.: Contribution of mass-dependent fractionation to the oxygen isotope anomaly of atmospheric nitrous oxide, J. Geophys. Res.-Atmos., 109, D03305, doi:10.1029/2003JD004088, 2004.

Kaiser, J., Hastings, M. G., Houlton, B. Z., Rockmann, T., and Sigman, D. M.: Triple oxygen isotope analysis of nitrate using the denitrifier method and thermal decomposition of N_2O, Anal. Chem., 79, 599–607, 2007.

Königer, P., Marshall, J. D., Link, T., and Mulch, A.: An inexpensive, fast, and reliable method for vacuum extraction of soil and plant water for stable isotope analyses by mass spectrometry, Rapid Commun. Mass. Sp., 25, 3041–3048, 2011.

Kool, D. M., Wrage, N., Oenema, O., Dolfing, J., and Van Groenigen, J. W.: Oxygen exchange between (de) nitrification intermediates and H_2O and its implications for source determination of NO3- and N_2O: a review, Rapid Commun. Mass. Sp., 21, 3569–3578, 2007.

Kool, D. M., Wrage, N., Oenema, O., Harris, D., and Van Groenigen, J. W.: The O-18 signature of biogenic nitrous oxide is determined by O exchange with water, Rapid Commun. Mass. Sp., 23, 104–108, 2009.

Lewicka-Szczebak, D., Well, R., Koster, J. R., Fuss, R., Senbayram, M., Dittert, K., and Flessa, H.: Experimental determinations of isotopic fractionation factors associated with N_2O production and reduction during denitrification in soils, Geochim. Cosmochim. Ac., 134, 55–73, 2014.

Lewicka-Szczebak, D., Well, R., Bol, R., Gregory, A., Matthews, P., Misselbrook, T., Whalley, R., and Cardenas, L.: Isotope fractionation factors controlling isotopocule signatures of soil-emitted N_2O produced by denitrification processes of various rates, Rapid Commun. Mass. Sp., 29, 269–282, 2015.

BGD
12, 17009–17049, 2015

Maeda, K., Spor, A., Edel-Hermann, V., Heraud, C., Breuil, M. C., Bizouard, F., Toyoda, S., Yoshida, N., Steinberg, C., and Philippot, L.: N_2O production, a widespread trait in fungi, Sci. Rep.-UK, 5, 9697, doi:10.1038/srep09697, 2015.

Mariotti, A., Germon, J. C., Hubert, P., Kaiser, P., Letolle, R., Tardieux, A., and Tardieux, P.: Experimental determination of nitrogen kinetic isotope fractionation – some principles – illustration for the denitrification and nitrification processes, Plant Soil, 62, 413–430, 1981.

Michalski, G., Scott, Z., Kabiling, M., and Thiemens, M. H.: First measurements and modeling of Delta O-17 in atmospheric nitrate, Geophys. Res. Lett., 30, 1870, doi:10.1029/2003GL017015, 2003.

Mohn, J., Wolf, B., Toyoda, S., Lin, C. T., Liang, M. C., Bruggemann, N., Wissel, H., Steiker, A. E., Dyckmans, J., Szwec, L., Ostrom, N. E., Casciotti, K. L., Forbes, M., Giesemann, A., Well, R., Doucett, R. R., Yarnes, C. T., Ridley, A. R., Kaiser, J., and Yoshida, N.: Interlaboratory assessment of nitrous oxide isotopomer analysis by isotope ratio mass spectrometry and laser spectroscopy: current status and perspectives, Rapid Commun. Mass. Sp., 28, 1995–2007, 2014.

Opdyke, M. R., Ostrom, N. E., and Ostrom, P. H.: Evidence for the predominance of denitrification as a source of N_2O in temperate agricultural soils based on isotopologue measurements, Global Biogeochem. Cy., 23, GB4018, doi:10.1029/2009GB003523, 2009.

Ostrom, N. E., Pitt, A., Sutka, R., Ostrom, P. H., Grandy, A. S., Huizinga, K. M., and Robertson, G. P.: Isotopologue effects during N_2O reduction in soils and in pure cultures of denitrifiers, J. Geophys. Res.-Biogeo., 112, G02005, doi:10.1029/2006JG000287, 2007.

Park, S., Perez, T., Boering, K. A., Trumbore, S. E., Gil, J., Marquina, S., and Tyler, S. C.: Can N_2O stable isotopes and isotopomers be useful tools to characterize sources and microbial pathways of N_2O production and consumption in tropical soils?, Global Biogeochem. Cy., 25, GB1001, doi:10.1029/2009GB003615, 2011.

Perez, T., Garcia-Montiel, D., Trumbore, S., Tyler, S., De Camargo, P., Moreira, M., Piccolo, M., and Cerri, C.: Nitrous oxide nitrification and denitrification ^{15}N enrichment factors from Amazon forest soils, Ecol. Appl., 16, 2153–2167, 2006.

Röckmann, T., Kaiser, J., Brenninkmeijer, C. A. M., and Brand, W. A.: Gas chromatography/isotope-ratio mass spectrometry method for high-precision position-dependent ^{15}N and ^{18}O measurements of atmospheric nitrous oxide, Rapid Commun. Mass. Sp., 17, 1897–1908, 2003.

BGD
12, 17009–17049, 2015

Rohe, L., Anderson, T.-H., Braker, G., Flessa, H., Giesemann, A., Lewicka-Szczebak, D., Wrage-Mönnig, N., and Well, R.: Dual isotope and isotopomer signatures of nitrous oxide from fungal denitrification – a pure culture study, Rapid Commun. Mass. Sp., 28, 1893–1903, 2014a.

Rohe, L., Anderson, T. H., Braker, G., Flessa, H., Giesemann, A., Wrage-Monnig, N., and Well, R.: Fungal oxygen exchange between denitrification intermediates and water, Rapid Commun. Mass. Sp., 28, 377–384, 2014b.

Schmidt, H. L., Werner, R. A., Yoshida, N., and Well, R.: Is the isotopic composition of nitrous oxide an indicator for its origin from nitrification or denitrification? A theoretical approach from referred data and microbiological and enzyme kinetic aspects, Rapid Commun. Mass. Sp., 18, 2036–2040, 2004.

Scholefield, D., Hawkins, J. M. B., and Jackson, S. M.: Development of a helium atmosphere soil incubation technique for direct measurement of nitrous oxide and dinitrogen fluxes during denitrification, Soil Biol. Biochem., 29, 1345–1352, 1997.

Snider, D., Venkiteswaran, J. J., Schiff, S. L., and Spoelstra, J.: A new mechanistic model of d18O-N_2O formation by denitrification, Geochim. Cosmochim. Ac., 112, 102–115, 2013.

Snider, D. M., Schiff, S. L., and Spoelstra, J.: N-15/N-14 and O-18/O-16 stable isotope ratios of nitrous oxide produced during denitrification in temperate forest soils, Geochim. Cosmochim. Ac., 73, 877–888, 2009.

Stein, L. Y. and Yung, Y. L.: Production, isotopic composition, and atmospheric fate of biologically produced nitrous oxide, Annu. Rev. Earth Pl. Sc., 31, 329–356, 2003.

Sutka, R. L., Ostrom, N. E., Ostrom, P. H., Gandhi, H., and Breznak, J. A.: Nitrogen isotopomer site preference of N_2O produced by Nitrosomonas europaea and Methylococcus capsulatus Bath, Rapid Commun. Mass. Sp., 17, 738–745, 2003.

Sutka, R. L., Ostrom, N. E., Ostrom, P. H., Breznak, J. A., Gandhi, H., Pitt, A. J., and Li, F.: Distinguishing nitrous oxide production from nitrification and denitrification on the basis of isotopomer abundances, Appl. Environ. Microb., 72, 638–644, 2006.

Sutka, R. L., Adams, G. C., Ostrom, N. E., and Ostrom, P. H.: Isotopologue fractionation during N_2O production by fungal denitrification, Rapid Commun. Mass. Sp., 22, 3989–3996, 2008.

Toyoda, S. and Yoshida, N.: Determination of nitrogen isotopomers of nitrous oxide on a modified isotope ratio mass spectrometer, Anal. Chem., 71, 4711–4718, 1999.

Toyoda, S., Mutobe, H., Yamagishi, H., Yoshida, N., and Tanji, Y.: Fractionation of N_2O isotopomers during production by denitrifier, Soil Biol. Biochem., 37, 1535–1545, 2005.

BGD
12, 17009–17049, 2015

Toyoda, S., Yano, M., Nishimura, S., Akiyama, H., Hayakawa, A., Koba, K., Sudo, S., Yagi, K., Makabe, A., Tobari, Y., Ogawa, N. O., Ohkouchi, N., Yamada, K., and Yoshida, N.: Characterization and production and consumption processes of N_2O emitted from temperate agricultural soils determined via isotopomer ratio analysis, Global Biogeochem. Cy., 25, GB2008, doi:10.1029/2009GB003769, 2011.

Well, R. and Flessa, H.: Isotopologue enrichment factors of N_2O reduction in soils, Rapid Commun. Mass. Sp., 23, 2996–3002, 2009.

Well, R., Flessa, H., Xing, L., Ju, X. T., and Romheld, V.: Isotopologue ratios of N_2O emitted from microcosms with NH_4^+ fertilized arable soils under conditions favoring nitrification, Soil Biol. Biochem., 40, 2416–2426, 2008.

Westley, M. B., Popp, B. N., and Rust, T. M.: The calibration of the intramolecular nitrogen isotope distribution in nitrous oxide measured by isotope ratio mass spectrometry, Rapid Commun. Mass. Sp., 21, 391–405, 2007.

Zhou, Z. M., Takaya, N., Sakairi, M. A. C., and Shoun, H.: Oxygen requirement for denitrification by the fungus Fusarium oxysporum, Arch. Microbiol., 175, 19–25, 2001.

BGD
12, 17009–17049, 2015

Table 1. Exp 1 results: soil moisture (expressed as water filled pore space: WFPS), $N_2O + N_2$ production rate (expressed as mass of N as sum of N_2O and N_2 per mass of dry soil per time), ^{17}O excess in soil nitrate ($\Delta^{17}O(NO_3)$) and in N_2O ($\Delta^{17}O(N_2O)$) with calculated exchange with soil water (x), and oxygen isotopic signature ($\delta^{18}O$) of soil nitrate (NO_3^-), soil water (H_2O) and N_2O with calculated isotope ratio difference between soil water and N_2O ($\delta^{18}O(N_2O/H_2O)$). For samples with non-inhibited N_2O reduction the N_2O mole fraction (f (N_2O)) was taken into account to calculate the $\delta^{18}O$ unaffected by N_2O reduction ($\delta_0^{18}O(N_2O)$) and the respective $\delta_0^{18}O(N_2O/H_2O)$.

WFPS [%]	$N_2O + N_2$ production rate [$\mu g\,kg^{-1}\,h^{-1}$]	$\Delta^{17}O(NO_3^-)$ [‰]	$\Delta^{17}O(N_2O)$ [‰]	x [%]	$\delta^{18}O(NO_3)$ [‰]	$\delta^{18}O(H_2O)$ [‰]	$\delta^{18}O(N_2O)$ [‰]	f (N_2O)[a]	$\delta_0^{18}O(N_2O)$[b] [‰]	$\delta_0^{18}O(N_2O/H_2O)$ [‰]
Exp 1.1 a, loamy sand, 8 °C										
79	114	11.9 ± 0.6	0.4 ± 0.5	96.2 ± 4.7	38.8 ± 0.5	−9.2 ± 0.5	13.4 ± 0.2	0.84 ± 0.04	10.4	19.7 ± 0.5
79	107	11.9 ± 0.6	0.8 ± 0.4	93.1 ± 3.1	38.8 ± 0.5	−9.2 ± 0.5	10.4 ± 0.1	1	10.4	19.8 ± 0.5
80	125	11.9 ± 0.6	0.8 ± 0.2	92.7 ± 1.1	37.5 ± 0.5	−13.5 ± 0.5	8.4 ± 0.3	0.84 ± 0.04	5.4	19.1 ± 0.6
80	126	11.9 ± 0.6	0.3 ± 0.7	96.2 ± 3.4	37.5 ± 0.5	−13.5 ± 0.5	5.7 ± 0.0	1	5.7	19.4 ± 0.5
Exp 1.1b, loamy sand, 22 °C										
78	427	10.4 ± 0.8	0.4 ± 0.2	95.7 ± 1.8	42.6 ± 0.5	−9.2 ± 0.5	12.5 ± 0.2	0.85 ± 0.06	9.6	19.0 ± 0.5
79	362	10.4 ± 0.8	0.4 ± 0.0	96.4 ± 0.2	42.6 ± 0.5	−9.2 ± 0.5	9.5 ± 0.0	1	9.5	18.9 ± 0.5
79	429	10.4 ± 0.8	0.2 ± 0.1	98.2 ± 1.5	42.1 ± 0.5	−13.5 ± 0.5	7.5 ± 0.1	0.85 ± 0.06	4.7	18.4 ± 0.5
80	370	10.4 ± 0.8	0.5 ± 0.1	94.8 ± 0.5	42.1 ± 0.5	−13.5 ± 0.5	4.5 ± 0.1	1	4.5	18.3 ± 0.5
Exp 1.1 c, silt loam, 22 °C										
80	266	9.2 ± 1.3	0.0 ± 0.2	99.5 ± 0.9	31.8 ± 0.5	−2.6 ± 0.5	26.4 ± 0.1	0.57 ± 0.03	16.4	19.1 ± 0.5
81	257	9.2 ± 1.3	0.4 ± 0.1	95.3 ± 1.4	31.8 ± 0.5	−2.6 ± 0.5	15.9 ± 0.1	1	15.9	18.5 ± 0.5
82	271	9.2 ± 1.3	0.1 ± 0.2	98.6 ± 1.3	31.8 ± 0.5	−8.7 ± 0.5	20.7 ± 0.2	0.57 ± 0.03	10.8	19.7 ± 0.5
82	251	9.2 ± 1.3	0.4 ± 0.1	95.0 ± 1.5	31.8 ± 0.5	−8.7 ± 0.5	9.8 ± 0.1	1	9.8	18.7 ± 0.5
Exp 1.2 a, loamy sand, 22 °C										
78	126	3.4 ± 0.5	n.d.	n.d.	6.5 ± 0.5	−10.4 ± 0.5	6.3 ± 0.1	1	6.3	16.9 ± 0.5
66	112	3.4 ± 0.5	0.2 ± 0.3	92.6 ± 8.5	6.5 ± 0.5	−10.1 ± 0.5	6.9 ± 0.2	1	6.9	17.2 ± 0.5
52	50	3.4 ± 0.5	0.0 ± 0.3	95.8 ± 3.9	6.5 ± 0.5	−8.9 ± 0.5	7.6 ± 0.3	1	7.6	16.6 ± 0.6
79	161	3.4 ± 0.5	n.d.	n.d.	6.5 ± 0.5	−5.0 ± 0.5	10.5 ± 0.0	1	10.5	15.6 ± 0.5
64	102	3.4 ± 0.5	0.2 ± 0.2	92.7 ± 5.2	6.5 ± 0.5	−5.7 ± 0.5	11.6 ± 0.1	1	11.6	17.5 ± 0.5
52	74	3.4 ± 0.5	0.2 ± 0.2	94.5 ± 5.1	6.5 ± 0.5	−6.6 ± 0.5	10.7 ± 0.1	1	10.7	17.4 ± 0.5
81	158	−1.5 ± 0.9	n.d.	n.d.	3.3 ± 0.5	−5.0 ± 0.5	10.8 ± 0.2	1	10.8	15.9 ± 0.5
64	77	−1.5 ± 0.9	−0.2 ± 0.3	84.4 ± 23.3 [c]	3.3 ± 0.5	−5.7 ± 0.5	11.0 ± 0.0	1	11.0	16.8 ± 0.5
50	46	−1.5 ± 0.9	−0.4 ± 0.3	68.9 ± 19.3 [c]	3.3 ± 0.5	−6.6 ± 0.5	9.4 ± 0.5	1	9.4	16.1 ± 0.7
Exp 1.2 b, silt loam, 22 °C										
77	137	2.6 ± 0.4	0.2 ± 0.2	90.6 ± 7.3	3.2 ± 0.5	−8.1 ± 0.5	8.3 ± 0.1	1	8.3	16.5 ± 0.5
60	130	2.6 ± 0.4	0.2 ± 0.1	92.2 ± 3.7	3.2 ± 0.5	−7.1 ± 0.5	9.8 ± 0.1	1	9.8	17.1 ± 0.5
46	121	2.6 ± 0.4	0.1 ± 0.1	96.5 ± 4.3	3.2 ± 0.5	−5.9 ± 0.5	12.5 ± 0.2	1	12.5	18.6 ± 0.5
77	111	2.6 ± 0.4	−0.1 ± 0.1	99.1 ± 1.6	3.2 ± 0.5	−1.6 ± 0.5	15.1 ± 0.2	1	15.1	16.7 ± 0.6
62	132	2.6 ± 0.4	0.0 ± 0.1	98.4 ± 1.6	3.2 ± 0.5	−1.8 ± 0.5	15.2 ± 0.2	1	15.2	17.0 ± 0.5
49	106	2.6 ± 0.4	−0.2 ± 0.0	100.0 ± 1.8	3.2 ± 0.5	−2.0 ± 0.5	15.7 ± 0.3	1	15.7	17.7 ± 0.6
77	124	−1.3 ± 0.8	−0.3 ± 0.3	72.4 ± 25.7 [c]	−2.0 ± 0.5	−1.6 ± 0.5	15.1 ± 0.1	1	15.1	16.8 ± 0.5
63	133	−1.3 ± 0.8	−0.0 ± 0.4	98.7 ± 31.3 [c]	−2.0 ± 0.5	−1.8 ± 0.5	14.9 ± 0.1	1	14.9	16.8 ± 0.5
47	125	−1.3 ± 0.8	−0.3 ± 0.3	72.5 ± 22.7 [c]	−2.0 ± 0.5	−2.0 ± 0.5	15.9 ± 0.1	1	15.9	18.0 ± 0.5

[a] $c(N_2O)/[c\,(N_2) + c\,(N_2O)]$: based on parallel ^{15}N treatment (last sampling results).
[b] N_2O reduction not inhibited, the values are corrected taking into account product ratio and isotope fractionation, according to Rayleigh fractionation $^{18}\varepsilon$ (N_2/N_2O) values taken from Lewicka-Szczebak et al. (2014): −17.4 ‰ (see Sect. 2.5 for details).
[c] Results disregarded because of large errors which are due to too small ^{17}O excess in the substrate.

BGD
12, 17009–17049, 2015

Table 2. Exp 2 results: soil moisture (expressed as water filled pore space: WFPS), $N_2O + N_2$ production rate (expressed as mass of N as sum of N_2O and N_2 per mass of dry soil per time), ^{17}O excess in soil nitrate ($\Delta^{17}O(NO_3)$) and in N_2O ($\Delta^{17}O(N_2O)$) with calculated exchange with soil water (x) and oxygen isotopic signature ($\delta^{18}O$) of soil nitrate (NO_3), soil water (H_2O) and N_2O. All $\delta^{18}O(N_2O)$ values were corrected taking into account product ratio to calculate the $\delta^{18}O(N_2O)$ values unaffected by N_2O reduction ($\delta_0^{18}O$ (N_2O)) and the respective $\delta_0^{18}O(N_2O/H_2O)$.

WFPS [%]	$N_2O + N_2$ production rate [mg g^{-1} h^{-1}]	$\Delta^{17}O(NO_3^-)$ [‰]	$\Delta^{17}O(N_2O)$ [‰]	x [%]	$\delta^{18}O(NO_3^-)$ [‰]	$\delta^{18}O(H_2O)$ [‰]	$\delta^{18}O(N_2O)$ [‰]	$f(N_2O)$ [a]	$\delta_0^{18}O$ (N_2O) [b] [‰]	$\delta_0^{18}O$ (N_2O/H_2O) [‰]
Exp 2.1, sand										
73.6 ± 0.7	91	10.8 ± 0.3	2.7 ± 0.4	73.9 ± 4.2	34.3 ± 1.7	−8.6 ± 0.5	12.1 ± 0.2	0.95 ± 0.01	11.5 ± 0.2	20.2 ± 0.5
			2.6 ± 1.1	74.4 ± 11.0			11.0 ± 0.4	0.92 ± 0.01	10.0 ± 0.5	18.8 ± 0.7
Exp 2.2 loamy sand										
70.4 ± 0.9	49	11.9 ± 0.3	3.7 ± 0.4	66.9 ± 3.1	43.0 ± 2.4	−7.4 ± 0.5	18.4 ± 2.7	0.80 ± 0.05	15.7 ± 2.1	23.3 ± 2.2
			3.3 ± 0.2	71.2 ± 1.6			15.7 ± 0.9	0.83 ± 0.02	13.5 ± 0.7	21.0 ± 0.8
Exp 2.3 silt loam										
78.4 ± 1.9	80	11.3 ± 0.2	5.2 ± 0.2	52.0 ± 2.2	43.1 ± 2.3	−5.3 ± 0.5	43.8 ± 2.2	0.32 ± 0.03	29.4 ± 2.6	34.9 ± 2.6
			5.3 ± 0.1	50.4 ± 1.4			46.1 ± 3.9	0.29 ± 0.10	30.4 ± 0.2	35.9 ± 0.5
Exp 2.4 silt loam										
73.6 ± 1.8	52	12.1 ± 0.3	3.5 ± 0.5	69.9 ± 4.0	52.0 ± 3.3	−5.0 ± 0.5	30.1 ± 0.4	0.68 ± 0.02	25.4 ± 0.7	30.5 ± 0.9
			5.0 ± 0.5	56.3 ± 4.1			37.7 ± 4.1	0.63 ± 0.07	31.9 ± 4.3	37.1 ± 4.3
Exp 2.5 organic										
86.5 ± 1.8	743	7.8 ± 0.2	2.3 ± 1.1	68.1 ± 13.8	30.4 ± 0.6	−6.4 ± 0.5	26.4 ± 5.3	0.60 ± 0.02	20.0 ± 5.1	26.6 ± 5.1
			2.3 ± 0.8	68.2 ± 9.5			37.7 ± 2.9	0.51 ± 0.02	29.3 ± 3.3	36.0 ± 3.3
Exp 2.6 organic										
78.7 ± 0.4	1198	12.5 ± 0.7	1.1 ± 0.2	90.2 ± 1.8	43.6 ± 5.6	−6.7 ± 0.5	18.5 ± 0.0	0.82 ± 0.02	16.1 ± 0.2	22.9 ± 0.6
			2.3 ± 0.3	78.8 ± 3.0			25.6 ± 0.8	0.74 ± 0.05	21.9 ± 1.6	28.7 ± 1.7

[a] $c(N_2O)/[c(N_2) + c(N_2O)]$: based on direct GC measurements in N_2-free atmosphere.
[b] Initial $\delta^{18}O$ values of unreduced N_2O calculated according to Rayleigh fractionation, $^{18}\varepsilon$ (N_2/N_2O) values taken from Lewicka-Szczebak et al. (2015): −12‰ (see Sect. 2.5)

BGD
12, 17009–17049, 2015

Table 3. Isotopic fractionation factors calculated based on Exp 1 results with Eq. (12) (see text for details). Results presented separately for Exp 1.1 and 1.2 and mean values for both.

	ε_w [‰]	ε_n [‰]
Exp 1.1	17.44 ± 0.71	0.74 ± 0.70
Exp 1.2	17.50 ± 0.67	-0.39 ± 0.66
mean all	17.48 ± 0.66	0.03 ± 0.86

BGD
12, 17009–17049, 2015

Table 4. Oxygen fractionation model based on the results obtained ($\delta_0^{18}O(N_2O)$) and isotope exchange (x) determined by $\Delta^{17}O$ method) and ε_w = 17.5 ‰ determined from Exp 1 data (Table 3). Scenarios with varied ε_n values and x_{NIR} or x_{NOR} (fraction of isotope exchange associated with NIR or NOR) are compared. D is the difference between measured $\delta^{18}O$ of N_2O and the calculated $\delta^{18}O$ of N_2O in a particular scenario.

	Scenario 0: $x = x_{NIR}$ or x_{NOR} $\varepsilon_n = 0$ $\varepsilon_w = 17.5$ [‰]		Scenario 1: $x_{NIR} = x$; $x_{NOR} = 0$ ε_n fitted $\varepsilon_w = 17.5$ [‰]		Scenario 2: $x_{NIR} = 0$; $x_{NOR} = x$ ε_n fitted $\varepsilon_w = 17.5$ [‰]		Scenario 3: $x_{NIR} = x_{NOR}$ ε_n fitted $\varepsilon_w = 17.5$ [‰]	
	calculated $\delta^{18}O(N_2O)$ [‰]	D	ε_n	D	ε_n	D	ε_n	D
Exp 1.1a	**10.5**	0.2	**0.3**	0.00	**2.3**	0.00	**1.0**	0.00
	5.4	0.6	**1.2**	0.00	**16.0**	0.00	**5.3**	0.00
Exp 1.1b	**9.6**	0.1	**0.2**	0.00	**2.7**	0.00	**0.9**	0.00
	6.1	−1.2	**-2.3**	0.00	**-22.6**	0.00	**-8.6**	0.00
Exp 1.1c	**15.7**	0.2	**0.4**	0.00	**4.7**	0.00	**1.7**	0.00
	10.1	0.0	**0.1**	0.00	**0.6**	0.00	**0.2**	0.00
Exp 1.2a	**7.4**	−0.3	**-0.5**	0.00	**-3.7**	0.00	**-1.6**	0.00
	8.6	−0.8	**-1.5**	0.00	**-18.4**	0.00	**-6.2**	0.00
	11.5	0.3	**0.6**	0.00	**4.5**	0.00	**1.9**	0.00
	10.7	0.2	**0.3**	0.00	**2.7**	0.00	**1.0**	0.00
Exp 1.2b	**8.9**	−0.4	**-0.7**	0.00	**-4.0**	0.00	**-1.9**	0.00
	9.9	0.1	**0.2**	0.00	**1.7**	0.00	**0.7**	0.00
	11.3	1.4	**2.6**	0.00	**38.5**	0.00	**12.1**	0.00
	15.8	−0.7	**-1.3**	0.00	**-72.8**	0.00	**-12.5**	0.00
	15.5	−0.3	**-0.6**	0.00	**-19.3**	0.00	**-4.2**	0.00
	15.5	0.2	**0.4**	0.00	**0.0**	0.22	**0.0**	0.22
Exp 2.1	**15.8**	−4.0	**-6.2**	0.00	**-14.7**	0.00	**-10.0**	0.00
	15.6	−5.3	**-8.2**	0.00	**-19.9**	0.00	**-13.4**	0.00
Exp 2.2	**21.3**	−5.2	**-7.6**	0.00	**-15.0**	0.00	**-11.0**	0.00
	19.8	−6.1	**-9.1**	0.00	**-20.0**	0.00	**-14.1**	0.00
Exp 2.3	**27.3**	2.5	**3.2**	0.00	**4.9**	0.00	**4.0**	0.00
	27.8	3.0	**3.8**	0.00	**5.7**	0.00	**4.7**	0.00
Exp 2.4	**24.6**	1.1	**1.6**	0.00	**3.4**	0.00	**2.4**	0.00
	30.0	2.2	**2.9**	0.00	**4.8**	0.00	**3.8**	0.00
Exp 2.5	**17.4**	2.8	**4.2**	0.00	**8.5**	0.00	**6.2**	0.00
	17.4	12.2	**18.1**	0.00	**37.1**	0.00	**27.0**	0.00
Exp 2.6	**14.2**	2.2	**3.8**	0.00	**20.9**	0.00	**10.2**	0.00
	17.9	4.2	**6.8**	0.00	**19.1**	0.00	**12.2**	0.00

BGD
12, 17009–17049, 2015

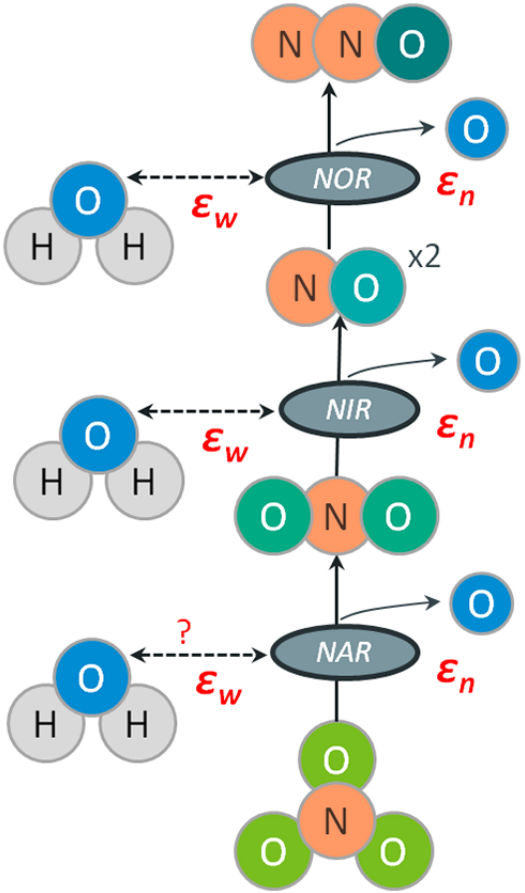

Figure 1. Oxygen isotope fractionation during denitrification as a result of branching effects (ε_n) und exchange effects (ε_w) associated with the following enzymatic reaction steps: NAR, NIR and NOR.

BGD
12, 17009–17049, 2015

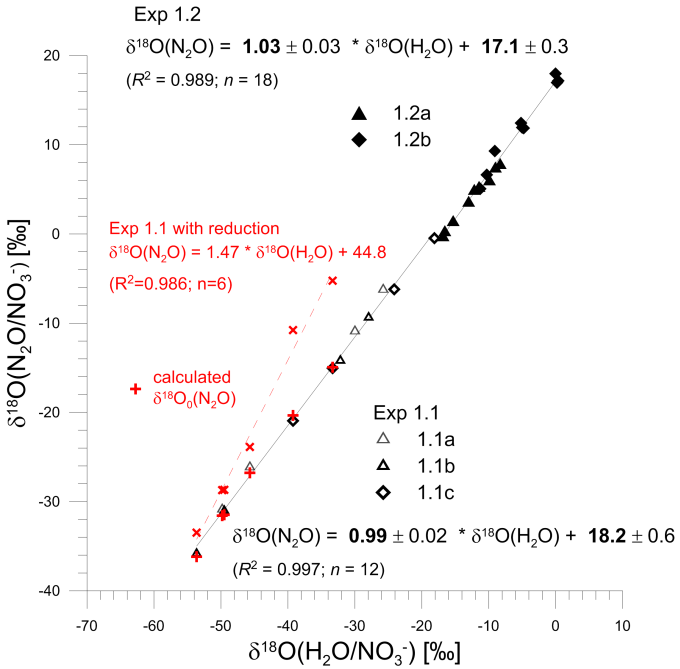

Figure 2. Correlation between oxygen isotopic signatures of N_2O and soil water expressed in relation to soil nitrate, the equation of linear fit allows for estimation of isotope exchange with soil water (slope of the linear fit) and the associated isotope effect (intercept of the linear fit). In red the influence of N_2O reduction on the method performance is presented – red X points represent the samples with not inhibited N_2O reduction (note that the slope and intercept are very different), whereas the red + points stand for the same samples after mathematical correction of N_2O reduction effect (as described in Sect. 2.5) which fit very well to the samples where N_2O reduction was inhibited. Data from Exp 1.

BGD
12, 17009–17049, 2015

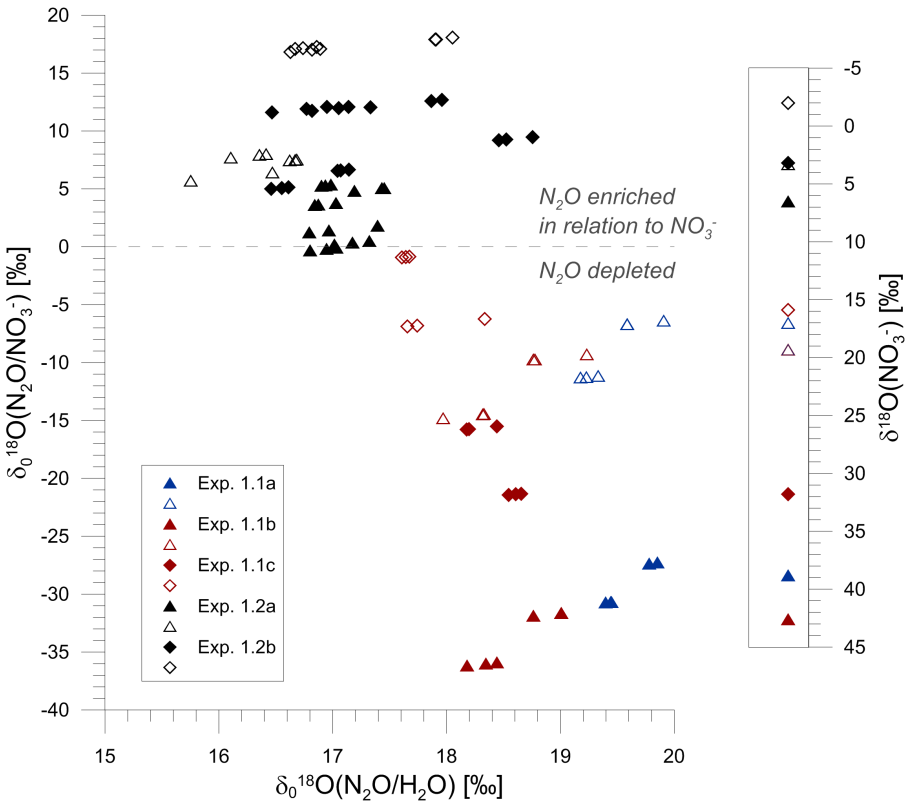

Figure 3. Relation between relative isotope ratio differences between produced N_2O and soil water ($\delta_0^{18}O(N_2O/H_2O)$ and between produced N_2O and soil nitrate ($\delta_0^{18}O(N_2O/NO_3^-)$, on the right $\delta^{18}O$ values of the initial soil nitrate for different treatments. $\delta^{18}O$ values of the initial soil water ranged between −13.5 and −1.6 ‰ (see Table 1) and its variation had no impact on $\delta_0^{18}O(N_2O/H_2O)$. Open symbols: addition of synthetic nitrate as fertilizer, filled symbols: addition of natural Chile saltpeter as fertilizer. Data from Exp 1.

BGD
12, 17009–17049, 2015

The mechanism of oxygen isotope fractionation

D. Lewicka-Szczebak et al.

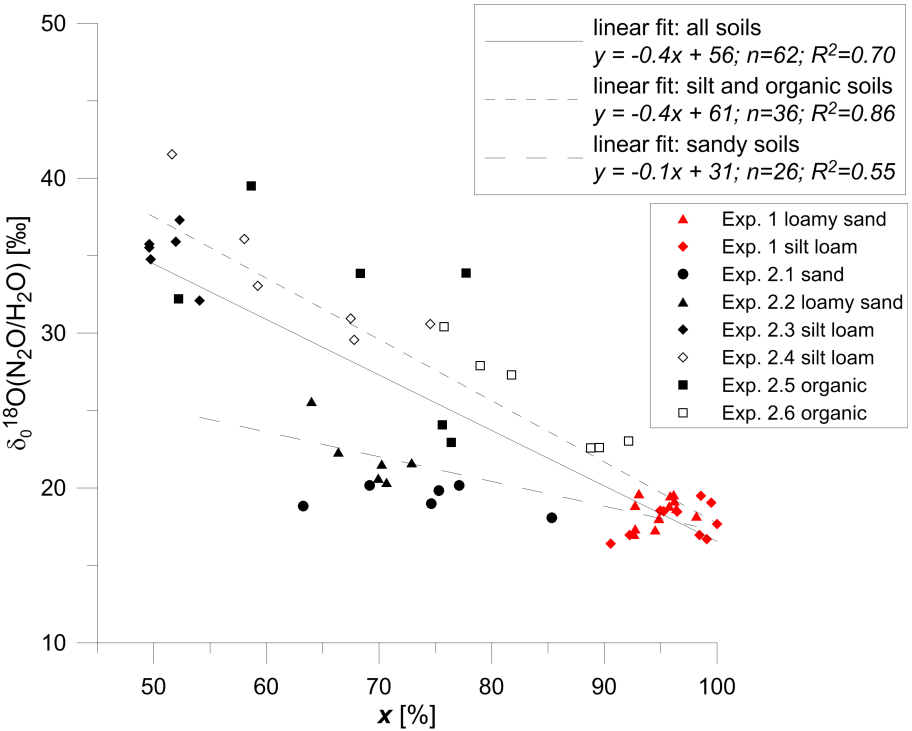

Figure 4. $\delta_0^{18}O(N_2O/H_2O)$ as a function of isotope exchange extent, x (determined with $\Delta^{17}O$ method). Red symbols: Exp 1, black symbols: Exp 2; open symbols: incubations with lower WFPS (70 %), filled symbols: incubations with higher WFPS (80 %). Note that same symbols shapes always represent the same soil.

BGD
12, 17009–17049, 2015

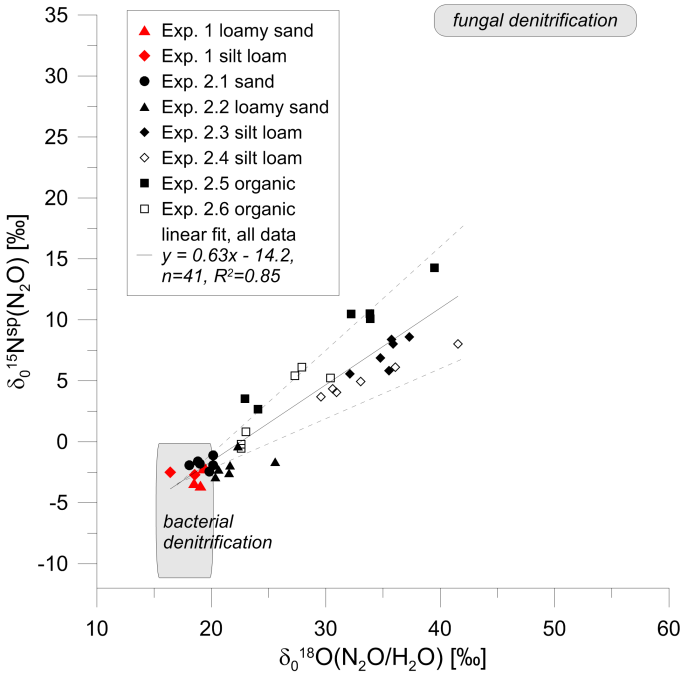

Figure 5. Relation between $\delta_0^{15}N^{sp}$ of produced N_2O and relative ratio difference between produced N_2O and soil water ($\delta_0^{18}O(N_2O/H_2O)$). Red symbols: Exp 1, black symbols: Exp 2; open symbols: incubations with lower WFPS (70 %), filled symbols: incubations with higher WFPS (80 %). Note that same symbols shapes always represent the same soil. Grey dashed lines represent the possible range of linear fit when extreme values of isotope effects for N_2O reduction are assumed in correction calculations (Eq. 5) – see discussion. Range of values for fungal denitrification from Rohe et al. (2014a).

BGD
12, 17009–17049, 2015